2009 MRS
spring meeting
San Francisco, CA · April 13-17

Fluidic Surface-Tension-Directed Self-Assembly of Miniaturized Semiconductor Dies Across Length Scales and 3D Topologies

Journal:	*2009 MRS Spring Meeting*
Manuscript ID:	578464
Symposium:	Symposium BB
Date Submitted by the Author:	06-Apr-2009
Complete List of Authors:	Knuesel, Robert; University of Minnesota, Department of Electrical and Computer Engineering Jacobs, Heiko
Keywords:	self-assembly, fluidics, soldering

Fluidic Surface-Tension-Directed Self-Assembly of Miniaturized Semiconductor Dies Across Length Scales and 3D Topologies

Robert J. Knuesel and Heiko O. Jacobs
Department of Electrical and Computer Engineering, University of Minnesota,
200 Union Street SE, Minneapolis, Minnesota 55455

ABSTRACT

This proceeding discusses recent progress on engineered fluidic surface-tension-directed self-assembly involving liquid solder. The process is applied to the assembly of discrete inorganic semiconductor device components at different length scales producing electrically interconnected devices and systems. Prior results include assembly with unique angular orientation and contact pad registration, parallel packaging, and the programmable assembly of various types of light emitting diodes. Recent progress on the scaling of the minimal die size from 300 to 30 µm is discussed which required the development of a new delivery system to concentrate and effectively introduce the components to solder-based receptors. Specifically, components are pre-oriented at a liquid-air or liquid-liquid interface and transferred onto the solder based receptors using a dynamic contact angle with a dipping process. Recent applications include the tiling of curved and 3D surfaces with single crystal semiconductors including the formation of flexible 3D solar cells.

INTRODUCTION

The construction of man-made artifacts such as cell phones and computers relies on robotic assembly lines that place, package, and interconnect a variety of devices that have macroscopic (>1 mm) dimensions [1]. The key to the realization of these systems is our ability to integrate/assemble components in 2D/3D as well as link/interconnect the components to transport materials, energy, and information. The majority of these systems that are on the market today are heterogeneous in nature. Heterogeneous systems can be characterized as systems that contain at least two separate parts, thereby prohibiting monolithic integration. Such systems are typically fabricated using robotic pick and place. The size of the existing systems could be reduced by orders of magnitudes if microscopic building blocks could be assembled and interconnected effectively [2]. The difficulty is not the fabrication of smaller parts, but their assembly into an interconnected system. For components with dimensions less than 100 µm, adhesive capillary forces often dominate gravitational forces, making it difficult to release the components from a robotic manipulator [3]. As a direct result, heterogeneous integration using an extension of serial robotic pick and place and wire-bonding has not proven a viable solution.

At the other extreme, nature forms materials, structures, and living systems by self-assembly on a molecular length scale [4, 5]. As a result, self-assembly based fabrication strategies are widely recognized as inevitable tools in nanotechnology and an increasing number of studies are being carried out to “scale-up” these concepts to close the assembly gap between nanoscopic and macroscopic systems. Recent demonstrations of processes that can assemble micrometer to millimeter-sized components include: shape-directed fluidic methods that assemble trapezoidal parts on planar surfaces on the basis of gravity and complementary 3D shapes [6, 7], liquid-solder-based self-assembly that uses the surface tension between pairs of molten solder drops to assemble functional systems [8-10], capillary force-directed self-assembly that uses hydrophilic/hydrophobic surface patterns and photo-curable polymers to integrate micro-optical components, micro-mirrors and semiconductor chips on silicon substrates [11-13], and sequential shape-and-solder-directed self-assembly that combines 3D shapes to define a chaperone with solder directed assembly to effectively assemble electrically interconnected parts [14-19]. The sequential shape-and-solder-directed self-assembly process has been applied to flip-chip assembly with unique contact pad registration [16] as well as the packaging of light emitting diodes [14-16] and transponders that can be interrogated remotely [17]. Comparing more recent concepts [18, 19] with the pioneering work by Yeh and Smith [6, 7], there are a number of fundamental differences: Recent methods do not require trapezoidal chips to prevent upside down assembly and asymmetric L or T shaped chip designs for angular orientation control. Instead they use simple shapes or openings in combination with solder coated areas to enable assembly in 3D or in 2D considering flip-chip assembly with unique angular orientation and contact pad registration. The openings are bigger than the components and act as guides for the solder directed self-assembly process. The solder drives the assembly into the aligned stable position and the driving force is surface tension, as opposed to gravity. Recent studies have also overcome the difficulty in assembling more than one component type through sequential methods that either use activation of selected receptors [20] or different sized openings [14-16]. Unique orientation no longer requires asymmetric three dimensional chips including triangular, L or T shaped parts that are not very common. While a number of applications have been demonstrated, scalability to smaller dimensions remains a challenge. Stauth et al. has successfully tested shape and solder directed self-assembly with 100 µm sized components [21], which are three times smaller than our previously reported parts [16]. This paper extends prior work [10, 14-16] in the area of shape and solder directed self-assembly to smaller scales. It reports on angular orientation control, flip-chip assembly, and recent progress in the assembly of ultra small chiplets with a side length of 20 µm. A new system employing a liquid-liquid interface will be presented to deliver and concentrate components with correct pre-orientation.

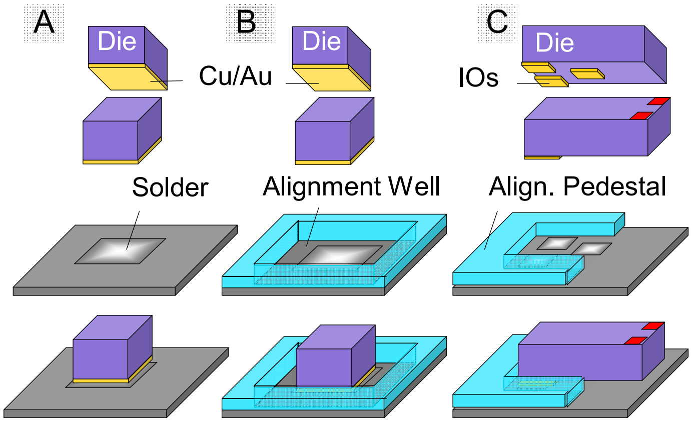

Figure 1
Self-assembly of dies using A) solder-based alignment alone, B) wells for size discrimination, and C) combined pedestals -, solder -, and IO - layouts that supports single-angle orientation and flip-chip contact pad registration.

Figure 1 illustrates the basic concept of solder directed self-assembly (Figure 1A) introducing alignment pedestals and contact pad layouts with increasing complexity. The layout shown in Figure 1B prevents assembly of more than one component type onto a single receptor, while the layout in Figure 1C enables flip-chip assembly with single-angle orientation and contact pad registration forming multiple contacts to the device: Components can only attach to the solder-coated areas if a correct angular pre-orientation condition is met. Components that arrive at the docking sites with an angular orientation that deviates by more than ±90° from the desired orientation will not find a sufficient overlap between the binding site (contact area) on the components and the solder-coated areas and therefore will not attach. Other components will be captured and aligned due to the reduction of the interfacial free energy.

EXPERIMENTS WITH COMPONENTS 300 μm – 3 mm IN SIZE

Figure 2 shows the sequential self-assembly procedure that we employ to batch-assemble differently sized components with a single-angle orientation. Following the large component assembly in Figure 2A, small components are assembled as in Figure 2B with complete differently sized component assembly shown in Figure 2C. When assembled in this order, large components will not assemble on the small docking sites due to the chaperone, while small components will be blocked from assembling on large docking sites by the previously assembled large components. The assembly was performed in a glass vial that was filled with ethylene glycol at a temperature of 150 °C so the solder was molten. Ethylene glycol was used to accommodate the higher melting point solder that is not compatible with a water-based assembly solution. We used both a low- (47 °C) and medium- (138 °C) melting-point (mp) solders (Y-LMA-117 and LMA-281, Small Parts, Miami Lakes, FL) in our experiments; we did not observe a notable difference between the two. The ethylene glycol solution was made slightly acidic (pH ~4.0) with hydrochloric acid to remove metal oxide from the surface of the solder drop; an oxide layer that — if sufficiently thick — blocked the wetting of the metal surface. Component transport and mixing was provided by hand agitation of the vial/drum to accomplish a tumbling motion across the surface, a motion that needs to be automated in future work.

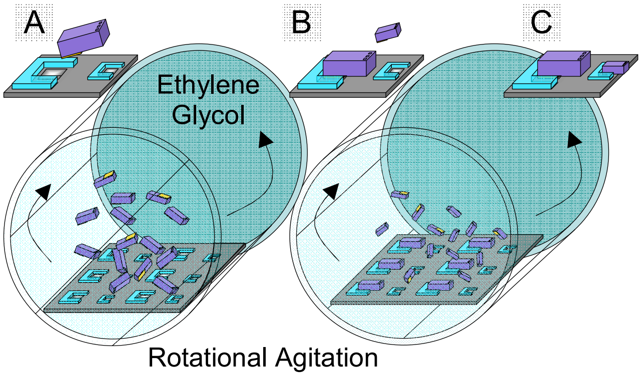

Figure 2
Rotational agitation procedure showing a two-step process to integrate multiple types of chiplets on a single substrate.

Through the course of this study we tested a number of different components including GaAlAs-LEDs, Si, glass, and SU-8 blocks with different pad layouts. Figure 3 represents a summary of the results. Figure 3A illustrates 1500 silicon chiplets, 300 μm on a side, which assembled onto a flexible polyimide surface with 98% coverage. With ~5000 components inside the vials, the assembly took about 90 s to reach steady state and was completed in 3 minutes. The lateral and angular precision was ~15 µm and ~3°, respectively, and limited by non-uniformity of the components that were fabricated by dicing using a dicing saw. Figure 3B shows GaAs/GaAlAs light-emitting diodes that have been assembled on a silicon substrate. The insets show the LEDs under operation. Without alignment pedestals, two chiplets can occupy a single receptor which is considered a defect. This defect can be eliminated using alignment pedestals as illustrated in Figure 3C. The entire assembly contained 196 interconnected LEDs with a side length of 280 µm. The chiplets assembled with four stable orientations 0°, 90°, 180°, and 270°. Figure 3D introduces unique angle orientation self assembly to reduce the number of stable orientations to one. A single-type component 10 × 10 array was assembled to determine alignment accuracy. The resulting accuracy of the self-assembly process was determined using the standard deviation which was 0.3° for the angular orientation and 19 µm for lateral accuracy. Figure 3E is an example of sequential batch assembly showing a 10×10 array that contains 900 µm and 500 µm sized dies assembled using a two-step self-assembly sequence. The largest components were 2×1×1 mm glass blocks. The blocks assembled with unique orientation and attached to 7 contacts on the substrate that are visible from the top (Figure 3F). The smallest components were 280 µm on a side (Figure 3C).

Figure 3 Summary of self-assembly results with varying docking site types using AlGaAs-LEDs, Si, Glass, and SU-8 blocks. A) Simple solder-directed assembly of silicon parts, B) simple solder-directed assembly of LEDs, C) well assembly, D) unique-angle orientation assembly, E) sequential batch assembly using "two-step" docking sites, and F) flip-chip assembly of parts with multiple IO connections.

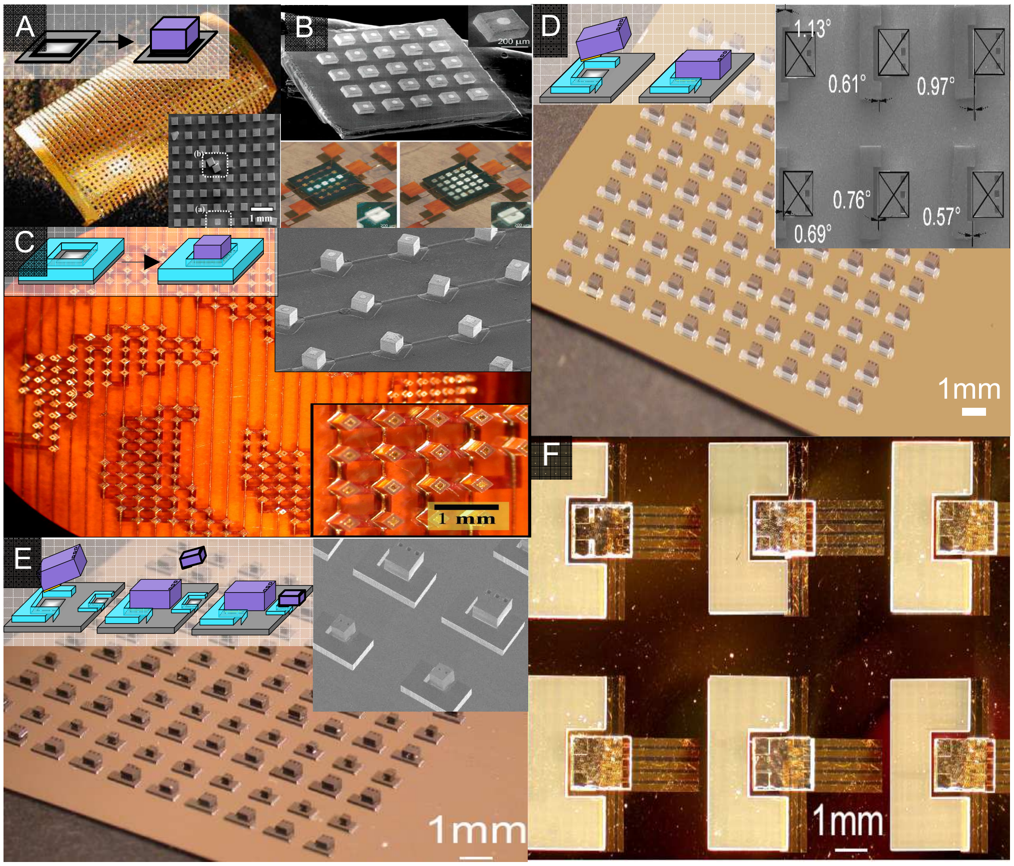

EXPERIMENTS WITH COMPONENTS 20 – 50 μm IN SIZE

It should be possible to scale down solder directed self-assembly to handle much smaller components than what has been demonstrated in Figure 3. The surface free energy of liquid solder dominates thermal energy and Brownian motion down to the sub-1 μm scale. In practice, however, scaling has been challenging. The problem is a surface oxide that forms due to residual oxygen, blocking the self-assembly. To combat this problem, small amounts of acid are added (pH 2-4) to the assembly solution. The acid addition, however, leads to an oxidative dissolution of the solder, an issue which becomes increasingly important as the solder volume is reduced. There are a number of potential solutions to this problem. In this study we present a new component delivery mechanism to speed up the self-assembly process by concentrating the number of available components. The process is illustrated in Figure 4.

Components are injected into the silicone oil and settle at the oil/water interface. We tested SU-8 and Si blocks that were formed through etching, carrying a single gold contact on one face. The components settle at the interface with the gold surface facing the water phase and the remainder facing the oil. The orientation can be defined using self-assembled monolayers (SAM) to render the surface of the gold hydrophilic (mercaptoundecanoic acid) and silicon hydrophobic (Dow Corning Z-6040 silane), for example. There has been a substantial body of work on self-assembly at the liquid-liquid interface that uses the static wetting angle between components to form free standing rafts and aggregates. The illustrated concept does not depend on or use the static wetting angle. Instead it makes use of the dynamic angle for a given liquid – liquid solid interface. The sheer velocity and viscosities determine the shape of the interface. Both up and downward slopes are possible as shown in Figure 4B. When the substrate is withdrawn from the liquid, the angle changes dramatically and components are delivered and concentrated in a thin surface layer. Depending on the preorientation, components can be assembled during either downward or upward motion. In the present study using the oil water interface, upward motion results in component delivery. During upward motion components get pushed towards the surface and touch the solder with metal coated faces causing a rapidly accelerated self-assembly when compared to experiments where the components are freely suspended in a solution. Figures 4A, C, and D show 20 μm SU-8 components that self-assembled after dipping the substrate ~10 times into the solution. Immersing the sample reverses the angle and removes unassembled components. This type of assembly is different to prior self-assembly at the liquid-liquid interface which aims at forming stable aggregates at the interface. While still forming a free standing raft of aggregated components at the interface, we now aim to transfer these components onto a solid substrate. The method has some similarity with Langmuir trough-type methods, but adds the use of liquid solder based receptors to order the components as they are transferred onto the substrate. The assembly also works at the air-water interface, however, introducing the air increases the level of oxidation, reducing assembly yields below the illustrated levels.

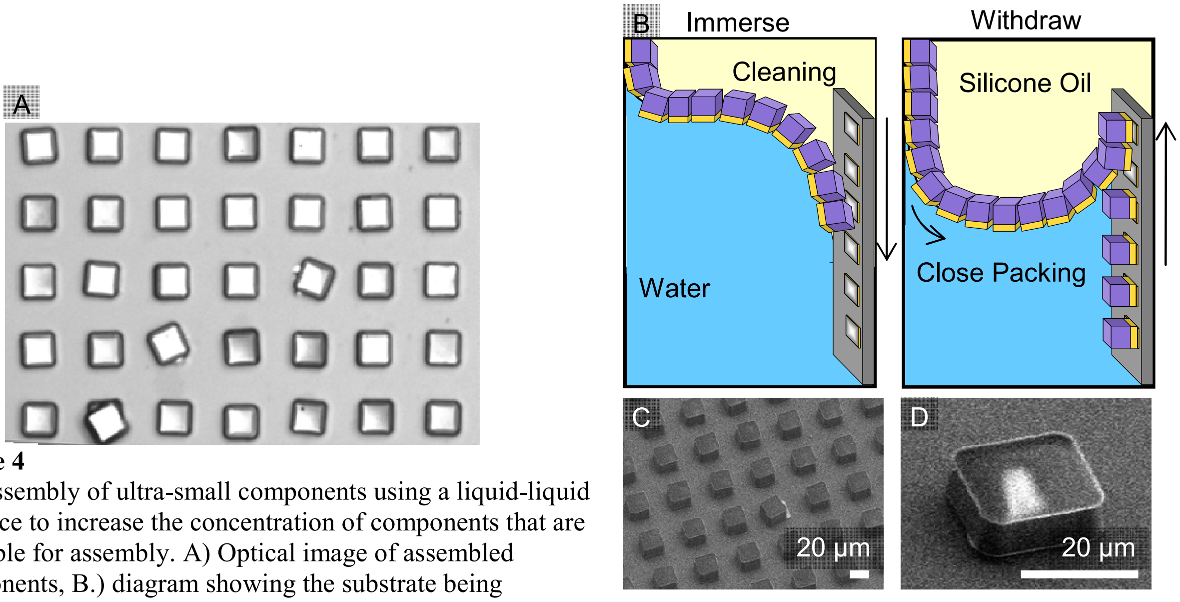

Figure 4
Self-assembly of ultra-small components using a liquid-liquid interface to increase the concentration of components that are available for assembly. A) Optical image of assembled components, B.) diagram showing the substrate being immersed and withdrawn from a silicone oil - water interface, and C, D) resultant scanning electron micrographs.

SEGMENTED FLEXIBLE MONTOCRYSTALLINE SOLAR CELL APPLICATION

A potential new application of fluidic self-assembly can be found in the manufacturing of solar cells on flexible substrates which could benefit from a reduction of material use and cost. To the best of our knowledge this has not yet been demonstrated in the literature. We report results of a segmented flexible solar cell formed by assembling doped monocrystalline silicon solar cell chiplets that are only 20 µm thick to reduce material use onto a 250 µm-thick flexible polyethylene terephthalate (PET) substrate to demonstrate the ability to assemble and electrically connect inorganic active devices in arbitrary patterns on non-planar and inexpensive substrates (Figure 5A). The process to complete the fabrication of the solar cell after self-assembly of the monocrystaline Si dies onto the substrate involves backfill with SU-8, etch to expose the top of the cells, and deposition of an ITO top contact. The resulting device showed no performance changes due to assembly or when flexed maintaining a >1 cm radius of curvature. Figure 5A when compared to Figure 4A depicts an improvement of the level of accuracy in the position and angular orientation. The improvement in yield and precision were a direct result of improving the accuracy in the dimensions of both the parts and the receptors. Figure 5B shows that besides the discrete assembly of dies with spacing in between them, it is possible to achieve closed packed arrays using a concept referred to as self-tiling whereby large solder areas become covered/tiled with smaller components. The solder surface tension encourages close packing while the greater pad geometry provides a long range order.

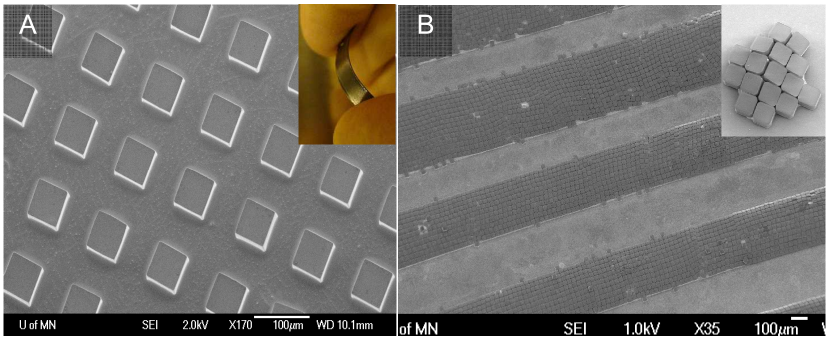

Figure 5
Extensions of ultra-small assembly, A.) Scanning electron micrograph of silicon solar cell chiplets assembled on a flexible PET substrate (shown in inset), and B.) Tiling of ultra-small components over very large areas. Surface tension draws the components into a close-packed arrangement as shown in the inset.

CONCLUSIONS

In summary, we have demonstrated examples of the directed self-assembly of micrometer-sized components with single-angular orientation accuracy of 0.3° and contact-pad registration for 280μm – 2mm sized dies. Alignment pedestals and registration to 7 contact pads has been shown providing a route to flip-chip self-assembly. Scaling down to 10-fold smaller chip dimensions, however, was not possible by a linear extension of the previous agitation concepts. Instead a new concept has been developed that makes use of a dynamic method that passes the chip through a liquid-liquid interface. This concept was applied to the assembly of monocrystalline silicon solar cell chiplets onto flexible and curved substrates, as well as the tiling of very large numbers of ultra-small chiplets onto large pads in a highly ordered way.

REFERENCES

[1] M. B. Cohn, K. F. Bohringer, J. M. Noworolski, A. Singh, C. G. Keller, K. Y. Goldberg, R. T. Howe, *Proceedings of SPIE* **1998**, *3512*, 2.
[2] T. D. Clark, J. Tien, D. C. Duffy, K. E. Paul, G. M. Whitesides, *Journal of the American Chemical Society* **2001**, *123*, 7677.
[3] R. S. Fearing, *Proceedings* **1995**, 212.
[4] S. Zhang, *Nature Biotechnology* **2003**, *21*, 1171.
[5] G. M. Whitesides, B. Grzybowski, *Science* **2002**, *295*, 2418.
[6] H. J. J. Yeh, J. S. Smith, *IEEE Photonics Technology Letters* **1994**, *6*, 706.
[7] J. S. Smith, H. J. J. Yeh, *US Patent* **1998**, *5,824,186*.
[8] D. H. Gracias, J. Tien, T. L. Breen, C. Hsu, E. M. Whitesides, *Science* **2000**, *289*, 1170.
[9] M. Boncheva, D. H. Gracias, H. O. Jacobs, G. M. Whitesides, *Proc. Natl. Acad. Sci. USA* **2002**, *99*, 4937.
[10] H. O. Jacobs, A. R. Tao, A. Schwartz, D. H. Gracias, G. M. Whitesides, *Science* **2002**, *296*, 323.
[11] U. Srinivasan, D. Liepmann, R. T. Howe, *Journal of Microelectromechanical Systems* **2001**, *10*, 17.
[12] U. Srinivasan, M. A. Helmbrecht, C. Rembe, R. S. Muller, R. T. Howe, *IEEE Journal of Selected Topics in Quantum Electronics* **2002**, *8*, 4.
[13] K. F. Böhringer, U. Srinivasan, R. T. Howe, Interlaken, Switzerland, **2001**.
[14] W. Zheng, P. Buhlmann, H. O. Jacobs, *Proc. Natl. Acad. Sci. USA* **2004**, *101*, 12814.
[15] W. Zheng, H. O. Jacobs, *Applied Physics Letters* **2004**, *85*, 3635.
[16] W. Zheng, H. O. Jacobs, *Advanced Functional Materials* **2005**, *15*, 732.

[17] F. Patolsky, G. Zheng, C. M. Lieber, *Analytical Chemistry* **2006**, *78*, 4260.
[18] H. O. Jacobs, Z. Wei, USA, Provisional Application, **March 2006**.
[19] C. R. Barry, H. O. Jacobs, *Nano Letters* **2006**, *6*, 2790.
[20] X. Xiong, Y. Hanein, J. Fang, Y. Wang, W. Wang, D. T. Schwartz, K. F. Bohringer, *Journal of Microelectromechanical Systems* **2003**, *12*, 117.
[21] S. A. Stauth, B. A. Parviz, *Proceedings of the National Academy of Sciences of the United States of America* **2006**, *103*, 13922.